Studies on Heterogeneous Degradation of Polypropylene/Talc Composite: Effect of Iron Impurity on the Degradation Behavior

Hisayuki Nakatani,[1] Hiroshi Shibata,[1] Kensuke Miyazaki,[1] Tetsu Yonezawa,[2] Hidetoshi Takeda,[3] Yutaka Azuma,[4] Shin Watanabe[5]

[1]Department of Biotechnology and Environmental Chemistry, Faculty of Engineering, Kitami Institute of Technology, Kitami, Hokkaido 090-8507, Japan
[2]Department of Chemistry, Graduate School of Science, The University of Tokyo, Bunkyo-ku, Tokyo 113-0033, Japan
[3]Advanced Technology Research Laboratories, Idemitsu Kosan Co., Ltd., Ichihara, Chiba 299-0193, Japan
[4]Composite Material Research Laboratory, CALP Corporation, Sodegaura-shi, Chiba 299-0205, Japan
[5]Suga Test Instruments Co., Ltd., Shinjuku-ku, Tokyo 160-0022, Japan

ABSTRACT: In this study, an effect of iron oxide (Fe_2O_3) impurity in talc on degradation behavior of polypropylene (PP)/talc composite was studied using a PP/Fe_2O_3 model composite sample. The thermal oxidative degradation was performed at 100°C. Although the degradation of a pure PP sample hardly occurred at such temperature, the existence of Fe_2O_3 induced the PP degradation. The degraded PP part was formed around the Fe_2O_3 grain in the PP/Fe_2O_3 sample. It was found from the optical microscope observation that the degraded PP was able to diffuse only within the PP amorphous part. The analysis of the oxidation distribution on the degraded PP surface was performed employing a scanning electron microscope/electron dispersive spectrometer. The result showed that the PP spots in the vicinity of the Fe_2O_3 grain were unoxidized during the initial degradation process, and the oxidized PP spots were located at around 6 μm distance from the Fe_2O_3 grain. It was concluded that the degradation was initiated microscopically away from the Fe_2O_3 grain so that the Fe_2O_3 had both the abilities to accelerate the decomposition of PP hydroperoxide compounds and to reduce the produced radical species into nonradical products. © 2009 Wiley Periodicals, Inc. J Appl Polym Sci 115: 167–173, 2010

Key words: polypropylene; talc; composite; iron oxide; heterogeneous degradation

INTRODUCTION

Polypropylene (PP) is widely applicable polymer material because of having many kinds of advantages such as easy processability and low production cost. However, the application has been somewhat limited due to the relatively poor stiffness. The composite with mineral has been considered a useful way to improve the stiffness. Talc has been widely used as the mineral for the composite. The PP/talc composite has been widely used as an industrial material.

The mechanical properties and the crystallization behavior of PP/talc composite have been widely studied by many researchers.[1–8] However, the degradation behavior has not been clarified yet.

The study on PP degradation has been generally performed with molten and/or molten-like states.[9–13] In these states, the degradation behavior follows classical kinetics with a homogeneous process. However, PP materials are generally exposed to mild conditions such as sunshine and lower temperature exposures. In these cases, the degradation occurs in the solid state,[14–19] and its degradation process is mainly heterogeneous. The heterogeneous degradation behavior is considerably complicated due to permeability of light, heat, oxygen, and diffusibility of degradation initiator.[15–19] Moreover, in the case of PP/talc composite, effects of talc on PP degradation should be considered because metallic compounds, which are constituents and impurity of talc, have an ability to accelerate the degradation.[20]

Recently, Hirano et al. reported heterogeneous degradation behavior of PP/rubber/talc composite.[21,22] The feature of this degradation was a visible striped pattern caused by internally-initiated microvoids. The microvoids were generated by exposures to ultraviolet irradiation and/or elevating temperature. Addition component, such as talc, seemed to cause such heterogeneous degradation in the PP matrix.

Talc is composed of hydrated magnesium sheet-silicates with a theoretical formula of $Mg_3Si_4O_{10}(OH)_2$. In fact, it certainly contains some associated minerals which constitute the gangue (Fe_2O_3, Al_2O_3, and CaO).[23] Among the metal oxides in the talc (containing the gangue), in particular, Fe_2O_3 would have the highest ability of accelerating PP degradation.[20] The heterogeneous degradation is thought to be a local degradation and Fe_2O_3 impurity is believed to partially accelerate the degradation.

To elucidate the heterogeneous degradation of PP/talc composite, the local degradation behavior should be microscopically studied based on the morphology. It is known that there is a microscopic application, as a method of microscopically observing degraded (oxidized) PP part,[14] as degraded PP has polar groups, it is distinguishable from undegraded PP. Local degradation behavior can be visually observed by a microscopic application based on such characteristics of degraded PP.[14]

In this study, an effect of the Fe_2O_3 impurity on degradation behavior of PP/talc was studied using a PP/Fe_2O_3 model composite sample. Our aim is to clarify the heterogeneous degradation behavior caused by the existence of Fe_2O_3 impurity. The behavior has been studied by a polarized optical microscope (POM) and a scanning electron microscope (SEM)/electron dispersive spectrometer (EDS).

EXPERIMENTAL

Materials

PP (meso pentad fraction = 98%) was supplied by Japan Polypropylene Co. (Yokkaichi, Japan). The number-average molecular weight (M_n) and the polydispersity (M_w/M_n) were 4.6×10^4 and 5.7, respectively. The PP was reprecipitated from a boiling xylene solution into ethanol and dried *in vacuo* at 60°C for 8 h. The PP obtained was sufficiently dried *in vacuo* and was used as samples without antioxidant.

Talc and Fe_2O_3 were purchased from Asada Milling and Kanto Chemical, respectively. They were used without further purification.

Preparations of PP and its composites

PP, PP/talc, and PP/Fe_2O_3 samples were prepared by an Imoto Seisakusyo IMC-1884 melting mixer. The melt mixing was performed using the purified PP without antioxidant. The melt mixing condition was 180°C at 60 rpm for 5 min. The samples were molded into a film (thickness: ca. 0.1 mm) by compression molding at 190°C under 4 MPa for 5 min and were quenched into water.
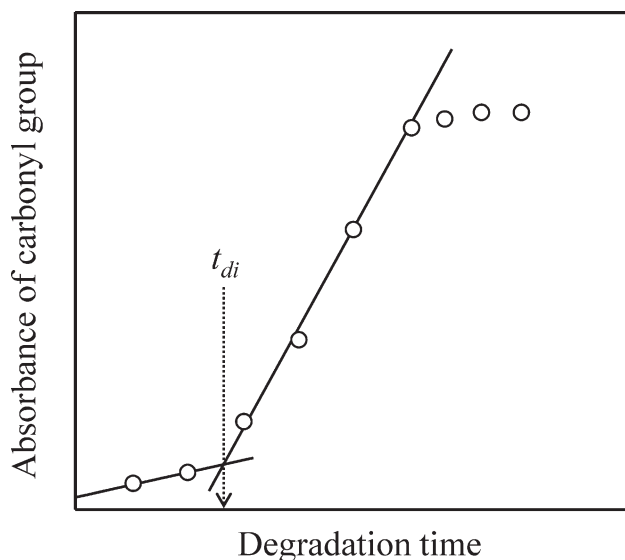
Figure 1 An example of carbonyl formation curve showing a determination of the duration of induction period (t_{di}).

X-ray fluorescence spectrometry (XRF) measurement

The metal composition of the talc was measured by XRF (Rigaku 3270) analysis using the PP (90 wt %)/talc (10 wt %) film.

Thermal oxidative degradation and calculation method of activation energy (E_a) using Fourier Transformed Infrared (FTIR) analysis

The film was put into a small vial and was allowed to stand in a heating block in air. The degraded film was measured by FTIR spectrometer (PerkinElmer Spectrum One). To evaluate the degradation rate, the duration of induction period (t_{di}) has been determined using the plots of the IR peak (carbonyl group: ca. 1715 cm^{-1}) intensity against the degradation time at several constant degradation temperatures. As illustrated in Figure 1, the t_{di} has been defined as the time (hour) at the intersection of the tangent at the inflection point with the plateau line of induction period. The E_a was calculated from the Arrhenius plot of the logarithm of t_{di} versus the reciprocal of temperature.

Preparations of thermal oxidative degraded PP (degPP) and of its mixture

The thermal oxidative degradation was carried out at 130°C for 18 h in air. The degraded PP was denoted as degPP ($M_n = 5.0 \times 10^3$, $M_w/M_n = 2.3$). The ^{1}H-NMR spectrum of degPP was measured using a JEOL ECX400 spectrometer (JEOL, Tokyo, Japan) at 120°C on 10% (w/v) solution in hexachloro-1,3-butadiene. 1,1,2,2-tetrachloroethane-d2 was
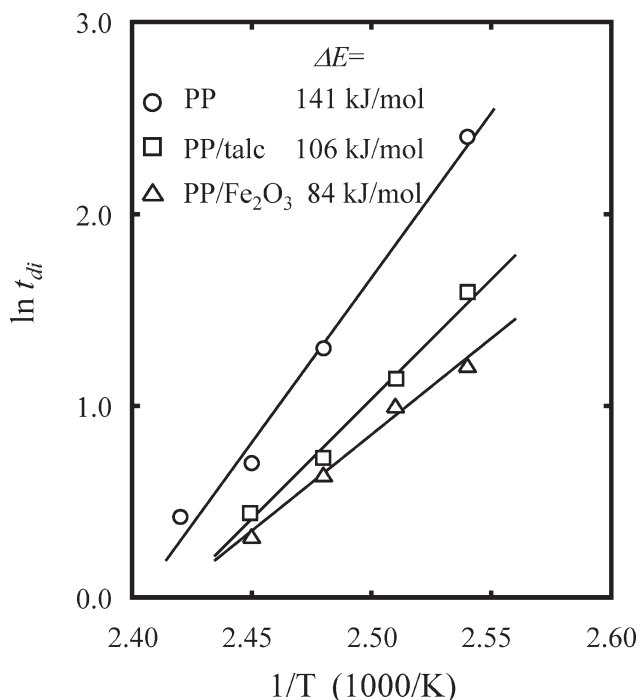
Figure 2 Arrhenius plots of t_{di} for thermal oxidative degradation of PP and PP composites. PP/talc = 90 wt %/10 wt %. PP/Fe$_2$O$_3$ = 98 wt %/2 wt %.

added as an internal lock and used as an internal chemical shift reference. The total content of oxidation compounds (γ-lactone and acid compounds) was calculated from the peak area between 2.1 and 2.3 ppm in the ^{1}H-NMR spectrum. The total content calculated from the area was ca. 1.6 mol %.

The mixture of PP (96.7 wt %) and degPP (3.3 wt %) was prepared by the Imoto Seisakusyo IMC-1884 melting mixer. The melt mixing was performed using the purified PP without antioxidant. The melt mixing condition was 180°C at 60 rpm for 5 min.

Spherulite observation

Spherulite observation was carried out with a Nikon ECLIPSE 50/POL POM. The isothermal crystallization temperature was controlled by a hot-stage system (Imoto Seisakusyo Microscopy Hot Stage). The film sample was heated in the hot stage and kept at 200°C for 5 min, and was quickly cooled to 130°C under nitrogen atmosphere. The growth of spherulite was isothermally performed at the constant temperature of 130°C.

Scanning electron microscope (SEM)/electron dispersive spectrometer (EDS) analysis

SEM analysis was carried out with a JEOL JSM-5800 at 30 kV. The plate of sample was fractured in liquid

nitrogen, and then the fractured surface was cut by the microtome to obtain the flat surface. The sample obtained was oxidatively degraded by an oven at 100°C and then was sputter-coated with gold. Iron, oxygen, and carbon contents were measured with an EDS (Oxford Instruments INCA Microanalysis).

RESULTS AND DISCUSSION

Figure 2 shows the Arrhenius plots of t_{di} for the thermal oxidative degradation of PP, PP (90 wt %)/talc (10 wt %) and PP (98 wt %)/Fe$_2$O$_3$ (2 wt %). The E_a of the degradation is evidently affected by the talc or the Fe$_2$O$_3$, and the order of decrease is as follows: Fe$_2$O$_3$ > talc > only PP. Although the additive amount of the Fe$_2$O$_3$ is less than that of the talc, the E_a is lower. This behavior suggests that the Fe$_2$O$_3$, which is the impurity in the talc, has played the main role in the acceleration of the PP degradation. In fact, the existence of Fe$_2$O$_3$ (ca. 0.18 wt % in all metal oxides) in this talc has been determined by XRF analysis.

Figure 3 shows the polarized optical micrographs of the nontreated and the treated PPs at the degradation temperature of 100°C for 24 h in air. The difference is unseen between these spherulite morphologies. This suggests that severe PP degradation, such as discoloration and/or crack, does not occur at this temperature for 24 h. In the case of the mixture of PP and degPP (see experimental section), as shown in Figure 4(a), there exist many black spots, corresponding to the discolored degPP. The cracks can be observed at the degradation temperature of 100°C [Fig. 4(b)] and propagate radially from these black spots. The propagation behavior suggests that the degradation growth has directivity. The degradation initiator such as radical species[24–26] cannot be diffused sufficiently in the crystalline part of PP at
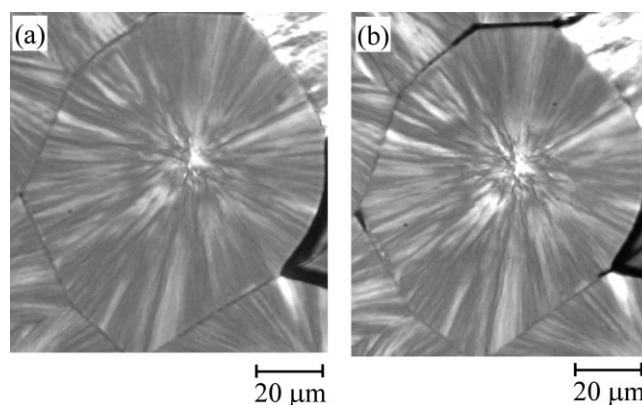

Figure 3 Polarized optical micrographs of PP. Isothermal crystallization at 130°C in nitrogen. Degradation condition; temperature = 100°C under air. (a) Degradation time = 0 h. (b) Degradation time = 24 h.
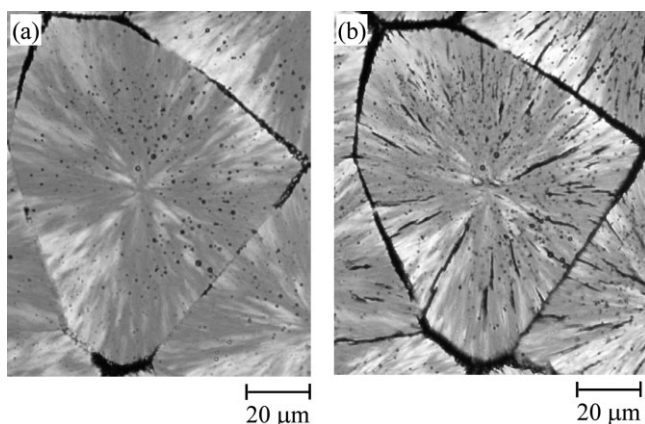
Figure 4 Polarized optical micrographs of mixture of PP (97 wt %) and DgPP (3 wt %). Isothermal crystallization at 130°C under nitrogen. Degradation condition; temperature = 100°C in air. (a) Degradation time = 0 h. (b) Degradation time = 24 h.

Figure 5 Polarized optical micrographs of PP/Fe$_2$O$_3$ (2 wt %) composite. Isothermal crystallization at 130°C under in nitrogen. Degradation condition; temperature = 100°C under air. (a) Degradation time = 0 h. (b) Degradation time = 24 h.

100°C.[27] Therefore, the degradation propagation concentrates in the amorphous part, which radially exists between the crystalline lamellae in the spherulite. In addition, the degPP is located preferentially in the amorphous phase because its crystallization rate is slower than that of PP. The degPP acts as the initiator due to the fact that it has some kind of oxidized compound in itself. Figure 4(b) suggests that the initiator can cause a local degradation of PP amorphous part even at a lower temperature.

Figure 5 shows the polarized optical micrographs of the nontreated and the treated PP/Fe$_2$O$_3$ (2 wt %) composites at the degradation temperature of 100°C for 24 h in air. The existence of many black spots corresponding to the Fe$_2$O$_3$ grains can be observed in the spherulite. It appears that Fe$_2$O$_3$ does not disturb the spherulite growth and also does not stimulate the generation as a nuclear agent of the
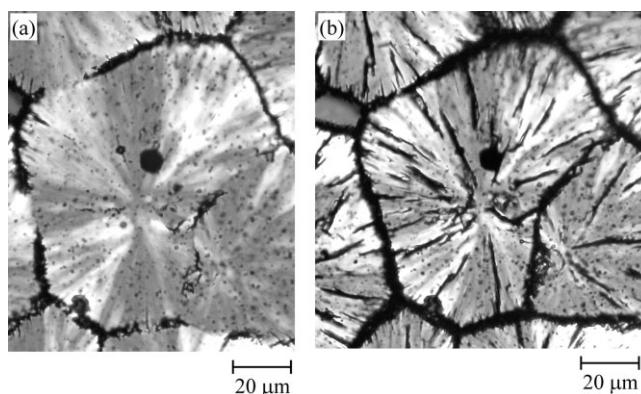
spherulite. As shown in Figure 5(b), the cracks originated from the Fe$_2$O$_3$ grains can be observed. The presence of Fe$_2$O$_3$ as well as degPP allowed the propagation of the degradation, even at 100°C.

It is known that the oxidative degradation of PP proceeds through a cycle reaction (autoxidation).[28–30] The hydroperoxide decomposition reaction is the rate-determining step in the autoxidation and is catalyzed by transition metal compounds.[20,31,32] However, the catalytic behaviour of the transition metals is considerably complicate. According to Black,[31] the transition metal suddenly changes to a potent inhibitor of autoxidation, when its concentration rises beyond a critical level. This catalyst-inhibitor transition would bring about unique degradation behavior in PP solid. In fact, Blakey and George[15] reported that Ti compounds stabilized PP in the immediate vicinity also formed reactive species, which acted as
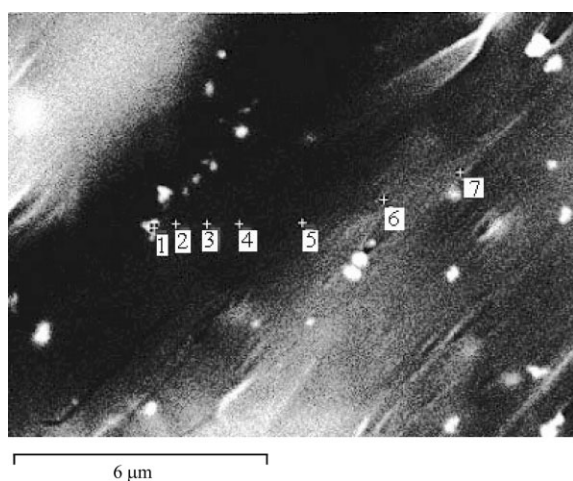
Spot	C	O	Fe
	[%]	[%]	[%]
1	94.81	3.22	1.97
2	99.55	0.20	0.25
3	99.11	0.79	0.10
4	99.77	0.00	0.23
5	99.82	0.00	0.18
6	99.71	0.02	0.27
7	99.01	0.00	0.99

Atomic percent.

Figure 6 SEM microphotograph of the surface of the oxidatively degraded PP (99.5 wt %)/Fe$_2$O$_3$ (0.5 wt %) composite at 100°C for 1 day and each sampling spot compositions measured by EDS analysis.
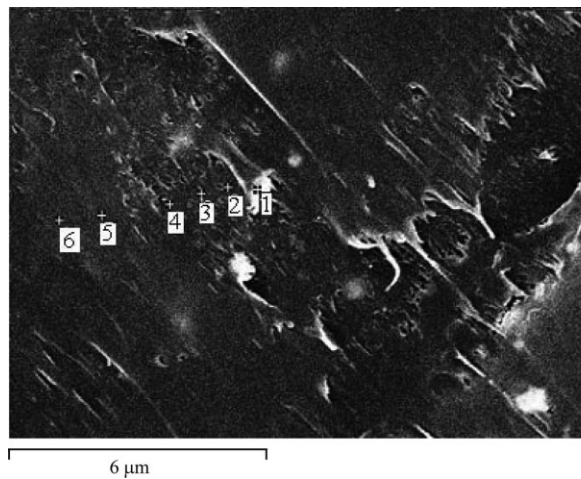
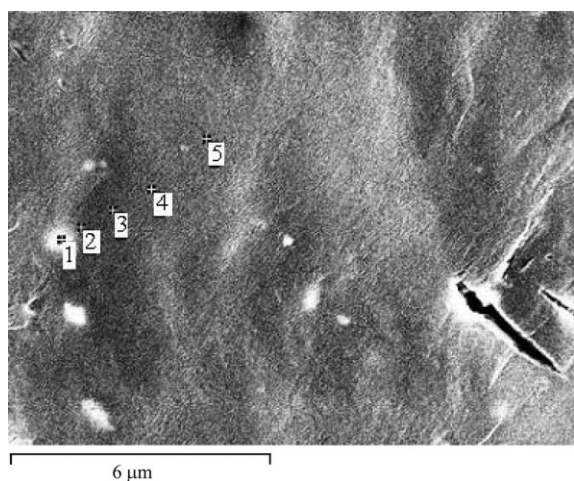| Spot	C [%]	O [%]	Fe [%]
1	88.31	7.09	4.61
2	99.91	0.00	0.09
3	99.52	0.00	0.48
4	98.64	0.79	0.57
5	96.49	3.14	0.37
6	94.83	4.62	0.54

Atomic percent.

Figure 7 SEM microphotograph of the surface of the oxidatively degraded PP (99.5 wt %)/Fe_2O_3 (0.5 wt %) composite at 100°C for 3 days and each sampling spot compositions measured by EDS analysis.

the PP degradation initiator at some places away from the Ti compounds. Therefore, the location of high Ti concentration was not microscopically corresponding to that of high degree of oxidation. The similar degradation behavior seems to occur in the PP/Fe_2O_3 composite, though it is not observed at the POM observation level.

To confirm whether Fe_2O_3 location is corresponding to the location of high degree of oxidation or not, the SEM/EDX analysis has been carried out with the PP/Fe_2O_3 composite containing a small amount (0.5 wt %) of Fe_2O_3. Figures 6, 7, and 8 show the SEM microphotographs of the PP (99.5 wt %)/Fe_2O_3 (0.5 wt %) at 100°C for 1, 3, and 4 days. The compositions of each sampling spots are measured by the EDS analysis in these figures. It should be noted here that the atomic percent ratio of O/Fe is approximately 1.5 at each spot number 1 in

these figures. This ratio means that there exists Fe_2O_3 grain at the spot number 1. In Figure 6, the oxygen contents are almost 0% at the other spots (numbers 2–7) as well as number 1, indicating that the degradation has hardly proceeded for 1 day. In the case of the 3 days, as shown in Figure 7, the oxygen contents are almost 0% at the spot numbers 2, 3, and 4 around 3 μm distance from the Fe_2O_3 grain (number 1). Whereas, the higher oxygen contents are observed around 6 μm distance (numbers 5 and 6) from the Fe_2O_3 grain. This heterogeneous behavior implies that the degradation is initiated microscopically away from the Fe_2O_3 grain. When the degradation proceeds for 4 days, the oxygen content becomes considerably higher at all spots as shown in Figure 8. In addition, an overall decrease of the carbon content and an overall increase of the iron content can be also observed. A number of Fe_2O_3

Spot	C [%]	O [%]	Fe [%]
1	65.59	20.76	13.65
2	62.87	29.35	7.77
3	68.20	20.63	11.17
4	50.07	44.77	5.15
5	46.08	53.92	0.00

Atomic percent.

Figure 8 SEM microphotograph of the surface of the oxidatively degraded PP (99.5 wt %)/Fe_2O_3 (0.5 wt %) composite at 100°C for 4 days and each sampling spot compositions measured by EDS analysis.
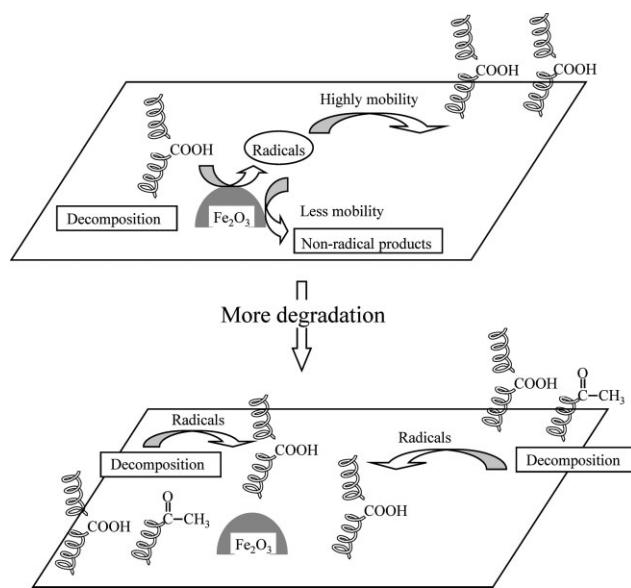
Figure 9 Schematical spreading model of degradation initiator in PP/Fe$_2$O$_3$ composite.

grains seem to appear at the surface by the volatilization of the PP matrix, suggesting that the degradation of the PP matrix proceeds severely.

The Fe$_2$O$_3$ accelerates the degradation of PP. In the oxidative degradation, the Fe$_2$O$_3$ catalytically decomposes the PP hydroperoxide compound and simultaneously stabilizes peroxy- and alkyl-radicals by converting to nonradical products as shown in eqs. (1) and (2).[15,31]

$$PO_2\bullet + Fe^{3+} \rightarrow Fe^{2+} + \text{non-radical products} \quad (1)$$

$$P\bullet + Fe^{3+} \rightarrow Fe^{2+} + \text{non-radical products} \quad (2)$$

If the radicals are formed around the Fe$_2$O$_3$ grain in the degradation process of the PP/Fe$_2$O$_3$, most parts of these radicals must be sequentially reduced to nonradical products by the Fe$_2$O$_3$. In particular, the less mobile radicals such as macroradical is likely reduced. On the other side, a part of highly mobile radicals can migrate away from the Fe$_2$O$_3$ grain and can initiate the remote oxidation (Fig. 9). The Fe$_2$O$_3$ stabilizes the PP matrix in the immediate vicinity but also forms the degradation initiator microscopically away from the Fe$_2$O$_3$. The unique initial degradation behavior can be interpreted by the complicated characteristics of the transition metal. When the degradation develops further, the amount of the hydroperoxide compound increases at some places away from the Fe$_2$O$_3$ grain. The increase leads to the reaction path of bimolecular hydroperoxide decomposition with a lower E_a[10,11] and is favorable for the spontaneous degradation. As shown in Figure 9, the radical species reproduced would gradually migrate

to the Fe$_2$O$_3$ grain and, the surroundings PP matrix would be finally oxidized (Fig. 8).

CONCLUSIONS

The effect of Fe$_2$O$_3$ impurity in talc on degradation behavior of PP/talc composite was studied using a PP/Fe$_2$O$_3$ model sample. The thermal oxidative degradation was performed at 100°C. Although the degradation of a pure PP sample hardly occurred at such temperature, the existence of Fe$_2$O$_3$ allowed the initiation of the PP degradation. The degraded PP part was formed around the Fe$_2$O$_3$ grain. The optical microscope observation showed that the degraded PP diffused within the amorphous part. In addition, the SEM/EDX analysis showed that the PP in the vicinity of the Fe$_2$O$_3$ grain was unoxidized in the initial degradation process, and the oxidized PP was located around 6 μm distance from it. It was found that the degradation was initiated microscopically away from the Fe$_2$O$_3$ grain so that the Fe$_2$O$_3$ had both the abilities to accelerate the decomposition of the PP hydroperoxide compounds and to reduce the produced radical species into nonradical products.

References

1. Maiti, S. N.; Sharma, K. K. J Mater Sci 1992, 27, 4605.
2. Taranco, J.; Martinez, J. M. G.; Laguna, O.; Collar, E. P. J Polym Eng 1994, 13, 287.
3. Martinatti, F.; Ricco, T. J Mater Sci 1994, 29, 442.
4. Švehlova, V.; Polouček, E. Angew Makromol Chem 1994, 214, 91.
5. Pukanszky, B.; Maurer, F. H. U. Polymer 1995, 36, 1617.
6. Obata, Y.; Sumitomo, T.; Ijitsu, T.; Masuda, M.; Nomura, T. Polym Eng Sci 2001, 41, 408.
7. Naiki, M.; Fukui, Y.; Matsumura, T.; Nomura, T.; Matsuda, M. J Appl Polym Sci 2001, 79, 1693.
8. Denac, M.; Musil, V.; Šmit, I. Compos Appl Sci Manuf 2005, 36, 1282.
9. Chien, J. C. W.; Wang, D. S. T. Macromolecules 1975, 8, 920.
10. Audouin, L.; Gueguen, V.; Tcharkhtchi, A.; Verdu, J. J Polym Sci Part A: Polym Chem 1995, 33, 921.
11. Achimsky, L.; Audouin, L.; Verdu, J.; Rychly, J.; Matisova-Rychla, L. J. Polym Degrad Stab 1997, 58, 283.
12. Audouin, L.; Achimsky, L.; Verdu, J. In Handbook of Polymer Degradation, 2nd ed.; Hamid, S. H., Eds.; Marcel Dekker: New York, 2000; p 727.
13. Tiemblo, P.; Gómez-Elvira, J. M.; Beltrán, S. G.; Matisova-Rychla, L.; Rychly, J. Macromolecules 2002, 35, 5922.
14. Billingham, N. C. Makromol Chem Macromol Symp 1989, 28, 145.
15. Blakey, I.; George, G. A. Polym Degrad Stab 2000, 70, 269.
16. Celina, M.; George, G. A. Polym Degrad Stab 1995, 50, 89.
17. Goss, B. G. S.; Nakatani, H.; George, G. A.; Terano, M. Polym Degrad Stab 2003, 82, 119.
18. Celina, M.; Clough, R. L.; Jones, G. D. Polymer 2005, 46, 5161.
19. Celina M, Clough, R. L.; Jones, G. D. Polym Degrad Stab 2006, 91, 1036.

20. Osawa, Z. Polym Degrad Stab 1988, 20, 203.
21. Hirano, K.; Tamura, S.; Kanai, T. J Appl Polym Sci 2007, 105, 2416.
22. Hirano, K.; Tamura, S.; Obata, Y.; Kanai, T. J Appl Polym Sci 2008, 108, 76.
23. Ahmed, M. M.; Ibrahim, G. A.; Hassan, M. M. A. Int J Miner Process 2007, 83, 132.
24. Celina, M.; George, G. A. Polym Degrad Stab 1993, 40, 323.
25. Celina, M.; George, G. A.; Billingham, N. C. Polym Degrad Stab 1993, 42, 335.
26. Celina, M.; George, G. A.; Lacey, D. J.; Billingham, N. C. Polym Degrad Stab 1995, 47, 311.
27. Tiemblo, P.; Gómez-Elvira, J. M.; Garcia Beltrán, S.; Matisova-Rychla, L.; Rychly, J. Macromolecules 2002, 35, 5922.
28. Achimsky, L.; Audouin, L.; Verdu, J.; Rychly, J.; Matisova-Rychla, L. Polym Degrad Stab 1997, 58, 283.
29. Audouin, L.; Gueguen, V.; Tcharkhtchi, A.; Verdu, J. J Polym Sci Part A: Polym Chem 1995, 33, 921.
30. Rychly, J.; Matisova-Rychla, L.; Csmorova, K.; Achimsky, L.; Audouin, L.; Tcharkhtchi, A.; Verdu, J. Polym Degrad Stab 1997, 58, 269.
31. Black, J. F. J Am Chem Soc 1978, 100, 527.
32. Filho, F. G. R.; Mélo, T. J. A.; Rabello, M. S.; Silva, S. M. L. Polym Degrad Stab 2005, 89, 383.